Journal of Cancer Research and Clinical Oncology
https://doi.org/10.1007/s00432-019-02870-x

ORIGINAL ARTICLE – CANCER RESEARCH

Iron oxide–gold core–shell nano-theranostic for magnetically targeted photothermal therapy under magnetic resonance imaging guidance

Ziaeddin Abed[1] · Jaber Beik[1] · Sophie Laurent[2] · Neda Eslahi[3] · Tahereh Khani[1] · Elnaz S. Davani[1] · Habib Ghaznavi[4] · Ali Shakeri-Zadeh[1,5]

Received: 15 December 2018 / Accepted: 19 February 2019
© Springer-Verlag GmbH Germany, part of Springer Nature 2019

Abstract

Recent efforts in the area of photothermal therapy (PTT) follow two important aims: (i) selective targeting of plasmonic nanoparticles to the tumor and (ii) real-time guidance of PTT operation through employing multimodal imaging modalities. In the present study, we utilized a multifunctional theranostic nanoplatform constructed from iron (III) oxide–gold (Fe_2O_3@Au) core–shell nanoparticles to fulfill these aims. The Au shell exhibits surface plasmon resonance, a property that is exploited to realize PTT. The magnetic core enables Fe_2O_3@Au to be employed as a magnetic resonance imaging (MRI) contrast agent. Furthermore, the magnetic core has the potential to establish a magnetic drug targeting strategy through which Fe_2O_3@Au can be directed to the tumor site by means of magnetic field. To test these potentials, Balb/c mice bearing CT26 colorectal tumor model were intravenously injected with Fe_2O_3@Au. Immediately after injection, a magnet was placed on the tumor site for 3 h to concentrate nanoparticles, followed by the near infrared (NIR) laser irradiation. MRI study confirmed the accumulation of nanoparticles within the tumor due to T2 enhancement capability of Fe_2O_3@Au. The in vivo thermometry results demonstrated that the tumors in magnetic targeting group had a significantly higher temperature elevation rate upon NIR irradiation than non-targeted group (~ 12 °C vs. 8.5 °C). The in vivo antitumor assessment revealed that systemic injection of Fe_2O_3@Au in combination with magnetic targeting and NIR irradiation resulted in complete remission of tumor growth. Therefore, Fe_2O_3@Au can establish a targeted PTT strategy for efficient eradication of tumor cells under the guidance of MRI.

Keywords Cancer · Photothermal therapy · Iron oxide–gold core–shell nanoparticles · Magnetic targeting · Magnetic resonance imaging

Introduction

Gold nanoparticles (AuNPs) are the most-commonly used light-responsive nanomaterial that have gained considerable attention in photothermal therapy (PTT) during last decade. When subjected to laser light, AuNPs are able to transform optical energy into heat, resulting in temperature rise of the surrounding medium. Therefore, preferential targeting of AuNPs to the tumor and then subsequent laser irradiation can realize a selective heat delivery strategy for thermal ablation of tumor cells (Abadeer and Murphy 2016; Eustis and El-Sayed 2006; Mirrahimi et al. 2019; Farashahi et al. 2019). The relatively short absorption wavelength of AuNPs of spherical shape in the visible region (~ 520 nm) is the major limitation of PTT, because the laser penetration depth is significantly limited due to strong absorption of light by tissue compositions such as hemoglobin and melanin.

✉ Habib Ghaznavi
dr.ghaznavi@zaums.ac.ir

✉ Ali Shakeri-Zadeh
shakeriz@iums.ac.ir

1 Finetech in Medicine Research Center, Iran University of Medical Sciences (IUMS), Tehran, Iran

2 General, Organic and Biomedical Chemistry, NMR and Molecular Imaging Laboratory, University of Mons, Mons, Belgium

3 Endometriosis Research Center, Iran University of Medical Sciences (IUMS), Tehran, Iran

4 Zahedan University of Medical Sciences (ZaUMS), Zahedan, Iran

5 Medical Physics Department, School of Medicine, Iran University of Medical Sciences (IUMS), Tehran, Iran

Published online: 07 March 2019

Near-infrared (NIR) region (700–1100 nm) is deemed to be an "optical therapeutic window" for PTT due to the minimal absorption of light by tissue (Qin and Bischof 2012). Therefore, the design and application of other structures of AuNPs such as nanoshells, nanorods and nanocages which are able to be tuned across the NIR region has been suggested as a possible solution to modify the penetration depth issue of PTT (Zhao et al. 2014; Tong et al. 2009; Chen et al. 2010).

The core–shell structure of iron oxide–gold nanoparticles (Fe_2O_3@Au) has been the result of recent research efforts to promote the applicability of PTT (Mirrahimi et al. 2018; Ghaznavi et al. 2018). The Au shell constitutes the light-responsive part of this nanocomplex than can be utilized in PTT. Meanwhile, the core–shell structure leads to a red-shift in the plasmon band, thereby enabling the use of NIR laser for photoactivation of this nanocomplex. The iron core of this nanocomplex on the other hand can be used as a negative contrast agent in T2-weighted magnetic resonance imaging (MRI). The magnetic core gives the ability to enhance the transverse relaxation rates of water protons, thereby creating hypointense signal areas at the spatial location of Fe_2O_3@Au, appearing as black spots on MR images (Eyvazzadeh et al. 2017). Moreover, the iron core enables a magnetic drug targeting (MDT) capability through which Fe_2O_3@Au can be directed to the desired location under an external magnetic field.

In previous efforts, we have highlighted the theranostic performance of Fe_2O_3@Au for photothermal ablation and MR imaging of cancer cells in vitro (Mirrahimi et al. 2018; Eyvazzadeh et al. 2017). In the present study, we attempt to take the full advantages of Fe_2O_3@Au to realize a targeted PTT under MRI guidance in vivo. For this purpose, CT26 colon tumor-bearing mice were injected with Fe_2O_3@Au and then subjected to an external magnetic field concentrated on the tumor site. The in vivo biodistribution of the nanoparticles was tracked through MRI to ensure that they were accumulated within the tumor. Next, mice were irradiated with NIR laser and the antitumor efficacy of this strategy was assessed through histological analysis and follow-up of tumor growth.

Materials and methods

Materials

Iron (II) chloride tetrahydrate (> 99%), iron (III) chloride hexahydrate (> 99%), ammonia (32%), hydrochloric acid (HCl), nitric acid (HNO_3), *N*-hydroxysuccinimide, dicyclohexylcarbodiimide were purchased from Merck (Darmstadt, Germany) for synthesis of nanoparticles. Dubelco's Modification of Eagle's Medium (DMEM) was purchased from GIBCO (Invitrogen, Germany). Fetal bovine serum (FBS) was purchased from BioSera Ltd. (Ringmer, United Kingdom). Trypsin-ethylenediaminetetraacetic acid (EDTA) and penicillin–streptomycin solution were purchased from Sigma-Aldrich Corp. (St Louis, MO, USA). All the materials were used for cell cultures.

Synthesis and characterization of Fe_2O_3@Au

The method for synthesis of Fe_2O_3@Au has been reported in our recent paper (Mirrahimi et al. 2018). Transmission electron microscopy (TEM; LEO906-ZEISS) was carried out to obtain information about the size and morphology of Fe_2O_3@Au. The hydrodynamic diameter of the nanoparticles in water was measured by dynamic light scattering (DLS, Zetasizer Nano ZS-90 instrument). The optical absorption spectra of Fe_2O_3@Au and AuNPs were also recorded using the Rayleigh UV-1601 instrument.

Tumor induction

CT26 cell line derived from mouse colon adenocarcinoma and male BALB/c mice (5–8 weeks old and weighing 20–25 g) were obtained from Pasteur Institute of Iran. Cells were cultured in RPMI 1640 medium with 10% FBS, 100 units/ml penicillin, and 100 µg/ml streptomycin at 37 °C in 5% CO_2. Cells were harvested by trypsinizing cultures with 1 mM EDTA/0.25% Trypsin (*w*/*v*) in PBS. After three passages, 2×10^6 CT26 cells suspended in 200 µl RPMI 1640 solution were injected subcutaneously on the right flank of BALB/c mice. All the animal experiments were conducted in accordance with guidelines established by the Institutional Animal Care Committee.

In vivo MRI study

The magnetic core of Fe_2O_3@Au enables to track the location of nanoparticles via MRI. Therefore, to determine the tumor localization of nanoparticles, mice were injected with nanoparticles via intratumoral (I.T) and intravenous (I.V) administration routes at the same concentrations as used in photothermal experiment (Sect. "In vivo antitumor experiments"). MRI examination was conducted at 30 min post I.T injection and 24 h post I.V injection. Moreover, to test the magnetic targeting capability of the nanoparticles, a magnet (magnetic field strength of 0.4 T) was placed on the tumor subsequent to I.V injection of nanoparticles for 3 h, and then the mice were imaged. These time intervals between nanoparticle injection and MRI imaging were optimized in a pilot MRI study, so that the nanoparticles showed maximum tumor accumulation at these time points. MRI study was performed using Philips superconductor clinical MR system (1.5 T) with the following acquisition parameter: T2*

weighted gradient echo, TR 250 ms, TE 11 ms, FA 25, slice thickness 2 mm and FOV of 386 mm × 248 mm.

In vivo antitumor experiments

The experiments were initiated when the tumor volume grew to approximately 100 mm^3. Mice were randomly divided into six groups ($n = 5$) and subjected to various treatments including: control (untreated), I.V injection of Fe_2O_3@Au [(Au): 1 mM, (Fe): 2 mM, 0.2 ml], NIR laser, I.T injection of Fe_2O_3@Au [(Au): 1 mM, (Fe): 2 mM, 0.05 ml] + NIR laser, I.V injection of Fe_2O_3@Au + NIR laser and I.V injection of Fe_2O_3@Au + MDT + NIR laser. The time intervals adopted between I.T and I.V injections of nanoparticles and laser irradiation were 30 min and 24 h, respectively. For magnetic targeting (MDT) group, immediately after I.V injection, a magnet was placed on the tumor site for 3 h to concentrate nanoparticles within the tumor, and thereafter the tumors were exposed to laser. For laser irradiation, mice were exposed to a continuous-wave 808 nm NIR laser source (Nanobon Company, Tehran, Iran) at the intensity of 1.4 W/cm^2 for 15 min. During laser irradiation, the temperature changes of the tumors were monitored in real-time using an infrared thermal imaging camera (Testo 875–1i, Germany). To estimate the antitumor effect of various treatments, the tumor volume changes were monitored during 28 days of study span. The tumor volume was calculated as: $\frac{\pi}{6} \times \text{length} \times (\text{width})^2$. The body weight and general condition of mice were also recorded during the treatment course. Moreover, histological examination of tumor tissue extracted from mice was performed at 48 h post-treatment using hematoxylin–eosin (H and E) staining.

Statistical methods

Statistical analysis was performed by one-way ANOVA test using SPSS software (version11). Then, the Tukey test at 95% confidence level was used as a post hoc test for pairwise comparison of means of the treatment groups. Measurement data are mean ± standard deviation (SD). A value of $P < 0.05$ was considered statistically significant.

Results

Characterization of Fe_2O_3@Au

As shown in Fig. 1a, TEM image of nanoparticles reveals that they have a magnetic core with the average diameter of 22 nm and Au shell with ~ 5 nm thickness uniformly covers the magnetic core. Hydrodynamic diameter of Fe_2O_3@Au measured by DLS shows that the effective diameter of nanoparticles is ~ 37 nm (Fig. 1b). Moreover, nanoparticles displayed a red-shift in the plasmon band with the peak absorption at 563 nm and a significantly higher absorption at the NIR region (700–1100 nm) than AuNPs (Fig. 1c).

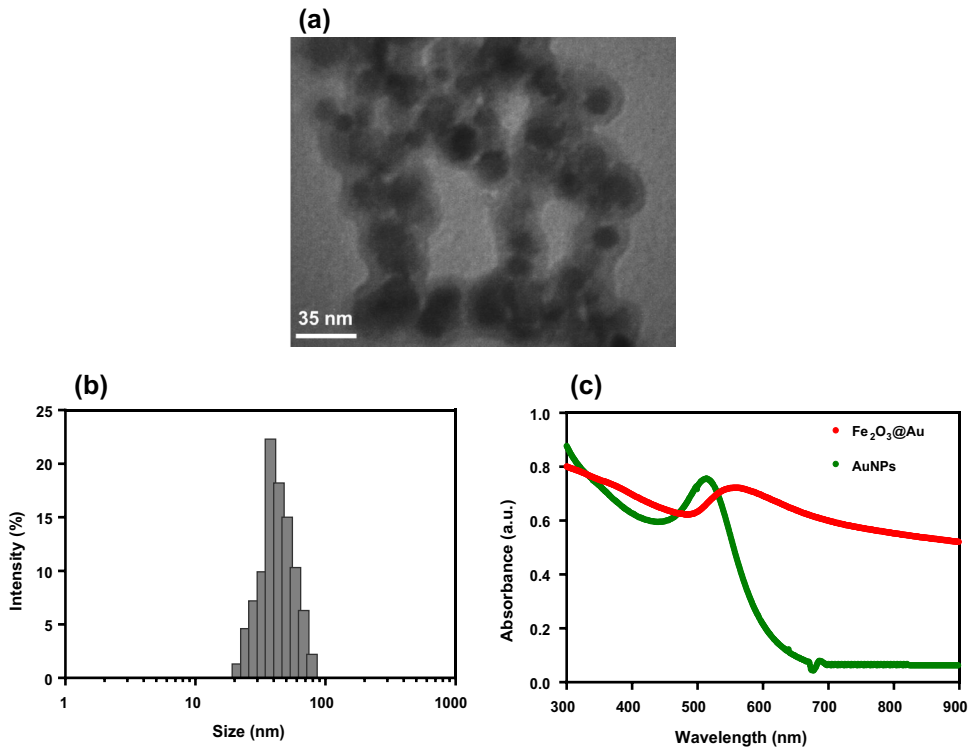

Fig. 1 Characterization of Fe_2O_3@Au nanoparticles. **a** TEM image and **b** size distribution histogram of Fe_2O_3@Au. The effective diameter of Fe_2O_3@Au is ~ 37 nm. **c** UV–Vis spectra of the solution of Fe_2O_3@Au and AuNPs. Fe_2O_3@Au shows a red-shift in the plasmon band with the absorption peak at 563 nm

In vivo MRI study

Firstly, the possibility to identify the in vivo localization of Fe_2O_3@Au through MRI was explored. As shown in Fig. 2a, I.T injection of Fe_2O_3@Au created markedly dark regions in the T2-weighted MR image of the tumor that validates the potential of this nanocomplex to be used as a negative MR contrast agent. Secondly, the tumor targeting capability of Fe_2O_3@Au under an external magnetic field was investigated. To this end, MR images of the tumor at 24 h post I.V injection and 3 h post I.V injection + MDT were compared. As shown in Fig. 2b, no hypointense area was observed on the MR image of the tumor following I.V injection, indicating that the accumulation of nanoparticles within the tumor is not enough to enhance T2 contrast. In contrast, I.V injection + MDT resulted in dark regions on the MR image (Fig. 2c), reflecting that Fe_2O_3@Au was effectively targeted to the tumor by external magnetic field and mainly accumulated under the surface of the tumor.

In vivo photothermal effect of Fe_2O_3@Au

Next, the photothermal effect of Fe_2O_3@Au was investigated by measuring the temperature variations of the tumor during laser irradiation using an infrared thermal camera. Laser irradiation alone for 15 min increased the tumor temperature by 5.5 °C, whereas I.V injection, I.V injection + MDT and I.T injection resulted in greater temperature rise of 8.5, 12 and 16.7 °C, respectively (Fig. 3). These results confirmed the photothermal effect of Fe_2O_3@Au, whereby they are able to convert NIR light into heat for thermal ablation of the tumor. Moreover, the higher temperature elevation rate of the tumor treated with I.V injection + MDT compared to I.V injection alone is another evidence, beside MRI study, that proved the enhanced tumor targeting efficiency of nanoparticles by means of magnetic field.

In vivo antitumor experiments

The photothermal ablation effect of Fe_2O_3@Au was explored by measuring the tumor volume changes after the mentioned treatments. As shown in Fig. 4a, NIR irradiation and I.V injection alone induced a slight inhibition in tumor growth compared to the control which was not statistically significant. I.V injection of Fe_2O_3@Au followed by NIR irradiation (24 h post-injection) delayed tumor growth and resulted in tumor inhibition rate of 66% (tumor inhibition rate $= 1 - \frac{V_{\text{treatment}}}{V_{\text{control}}}$; V stands for tumor volume). However, the tumors treated with I.T injection + NIR and I.V injection + MDT + NIR were completely eradicated within days after treatment and the mice remained healthy over 28 days of follow-up period without the evidence of recurrence. Representative photographs of the mice in Fig. 4b obviously indicates the antitumor efficacy of various treatments. Therefore, as expected from MR images of the mice and in vivo thermometry results, the more efficient accumulation of nanoparticles in the tumor due to magnetic targeting than I.V injection dramatically enhanced therapeutic response, so that I.V

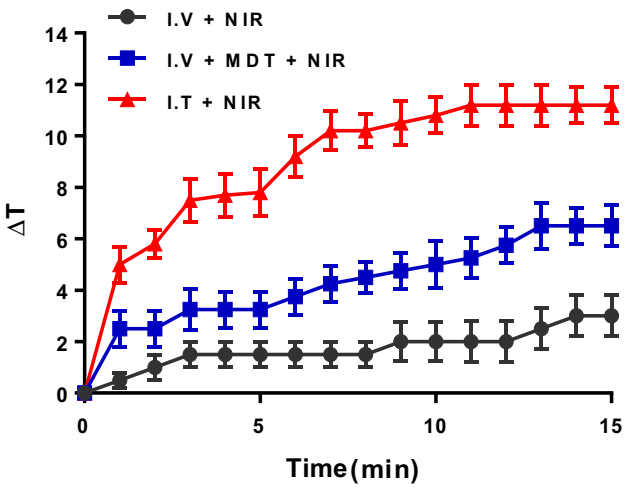

Fig. 3 In vivo tumor thermometry. Relative temperature rise of CT26 tumor injected with Fe_2O_3@Au during NIR irradiation (808 nm, 1.4 W/cm^2) compared to the tumor without nanoparticle injection. *NIR* near infrared laser, I.V and I.T intravenous and intratumoral injection of Fe_2O_3@Au, *MDT* magnetic targeting

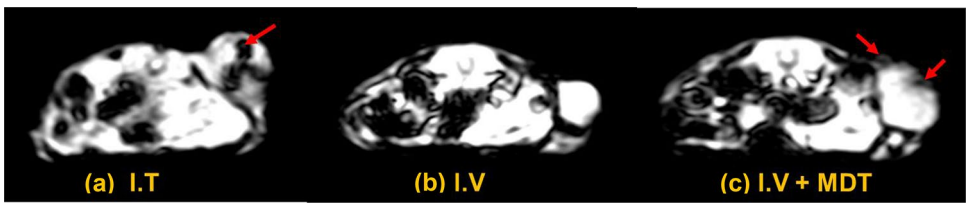

Fig. 2 In vivo MR imaging of CT26 tumor-bearing mice. T2-weighted MR images of mice at **a** 0.5 h post intratumoral (I.T) injection, **b** 24 h post intravenous (I.V) injection, and **c** 3 h post I.V injection followed by magnetic targeting (MDT) of Fe_2O_3@Au. The hypointense regions within the tumor represent the spatial location of nanoparticles, as indicated by arrow

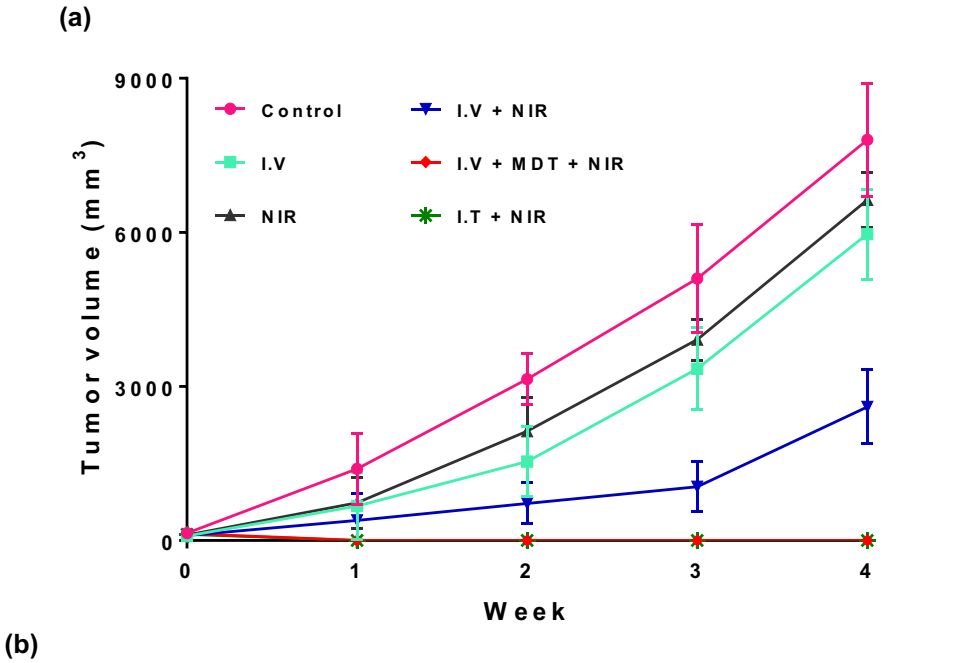

Fig. 4 In vivo antitumor assessment of Fe_2O_3@Au. **a** Tumor volume change and **b** representative photographs of CT26 tumor-bearing mice under various treatments. *NIR* near infrared laser, *I.V and I.T* intravenous and intratumoral injection of Fe_2O_3@Au, *MDT* magnetic targeting

injection + MDT + NIR exhibited an antitumor efficacy similar to that of I.T injection + NIR.

To determine whether the treatments are toxic to the mice, the body weight of mice was recorded during the study period. As shown in Fig. 5, in all treatment groups, mice were able to maintain their body weights, suggesting that Fe_2O_3@Au alone or in combination with laser is not toxic to the mice. The increase in body weight of mice over the treatment course was related to their growing tumor burden and normal body growth. Histological condition of tumor tissue was also investigated to further confirm the antitumor activity of Fe_2O_3@Au. As shown in Fig. 6, H and E staining reveals that the tumors treated with NIR and I.V injection of Fe_2O_3@Au show normal cell morphology and similar cell density to the control group. The tumor treated with I.V + NIR exhibits a decreased cell density and evidence of cell necrosis. In sharp contrast, a marked reduction in cell density and extensive areas of necrosis can be clearly seen in the tumor sections after treatment with I.V + MDT + NIR and I.T + NIR.

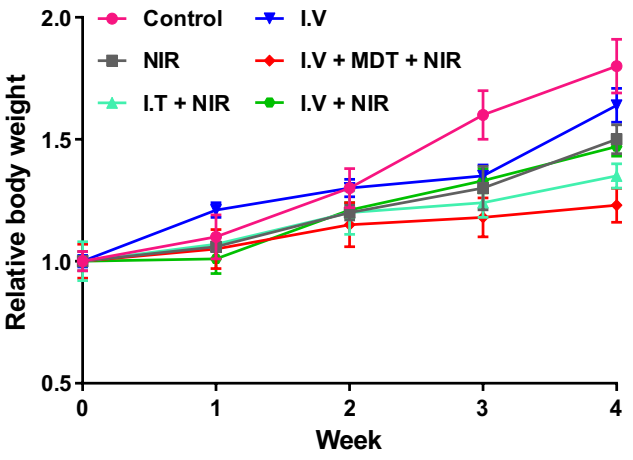

Fig. 5 In vivo toxicity assessment of Fe_2O_3@Au. The body weight change of CT26 tumor-bearing mice as a function of time post-treatment. *NIR* near infrared laser, *I.V and I.T* intravenous and intratumoral injection of Fe_2O_3@Au, *MDT* magnetic targeting

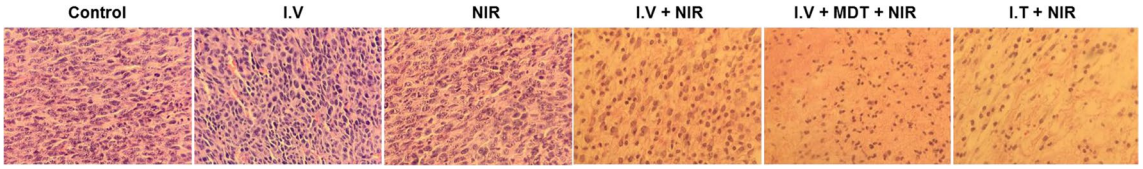

Fig. 6 Histological evaluation. Representative H&E images of CT26 tumor sections at 48 h post-treatment under various conditions. *NIR* near infrared laser, *I.V and I.T* intravenous and intratumoral injection of Fe_2O_3@Au, *MDT* magnetic targeting

Discussion

PTT using AuNPs has exhibited encouraging results in recent pre-clinical researches (Beik et al. 2017). Compared to traditional methods of hyperthermia such as radiofrequency-, microwave- and ultrasound-induced hyperthermia that leads to unwanted thermal damage to healthy tissue, PTT represents a precise heat delivery strategy for selective ablation of tumor cells (Manuchehrabadi et al. 2013; Beik et al. 2016, 2018 ; Shakeri-Zadeh et al. 2014; Bagher et al. 2018). Although PTT encounters with serious drawback of limited penetration depth of light, the use of light in the NIR wavelength region in association with NIR-responsive nanoparticles can be modified in this problem to some extent. AuroLase® is a FDA-approved NIR-responsive AuNPs formulation constructed of Au shell on silica core which has been evaluated in separate clinical trials for the PTT of head and neck (NCT00848042) and lung (NCT01679470) tumors.

In the previous report, we demonstrated the anticancer effect of PTT with Fe_2O_3@Au in vitro (Mirrahimi et al. 2018). Compared to commonly used spherical AuNPs which are tuned to the visible region, the as-developed nanoparticles displayed a red-shift in the surface plasmon band (absorption peak: 563 nm). This is a great advantage of Fe_2O_3@Au that makes them a well-suited NIR photothermal agent, thereby allowing a deeper seated tumor to be treated. Despite NIR absorption properties, the magnetic core of Fe_2O_3@Au enables them to be targeted toward a desired location under external magnetic field and also be tracked through MRI. As shown in Fig. 3, the tumor thermometry during PTT operation showed a negligible temperature enhancement due to systemic injection of Fe_2O_3@Au relative to NIR irradiation alone. MRI study proved that magnetic targeting is efficient to concentrate nanoparticles into the tumor (Fig. 2). As a result, magnetic targeting of Fe_2O_3@Au to the tumor and subsequent NIR irradiation led to a significantly higher temperature enhancement that non-targeted group. Enhanced accumulation of Fe_2O_3@Au by means of magnetic field and subsequent NIR irradiation eventually resulted in complete tumor eradication with no recurrence 28 days after treatment.

It is well-known that nanoparticles are able to passively accumulate and preferentially retain at the tumor through enhanced permeability and retention (EPR) effect which is the result of leaky vasculature and ineffective lymphatic drainage of the tumor tissue (Maeda et al. 2000). Passive targeting following systemic (I.V) administration, however, is a very heterogeneous phenomenon, varying dramatically from one tumor to another and from one patient to the next, resulting in ineffective tumor targeting (Jain and Stylianopoulos 2010; Hashemian et al. 2009; Shakeri-Zadeh et al. 2009). On the other hand, direct injection of nanoparticles into the tumor is not feasible in real clinical setting. One unanticipated finding of this study was that the antitumor effect of PTT with I.V injection of Fe_2O_3@Au followed by magnetic targeting was similar to that obtained after I.T injection of nanoparticles. Accordingly, the magnetic targeting of hybrid plasmonic magnetic nanoparticles can be suggested as an effective strategy to increase the intratumoral concentration of nanoparticles, thereby enhancing the therapeutic efficiency of PTT.

Conclusion

The current study aimed to extend the clinical utility of PTT by taking the advantages of theranostic Fe_2O_3@Au nanoparticles. MRI study revealed that Fe_2O_3@Au can be targeted to the tumor when subjected to external magnetic field. The enhanced tumor accumulation of nanoparticles due to magnetic targeting and subsequent NIR irradiation dramatically suppressed tumor growth. Therefore, the as-developed Fe_2O_3@Au has the potential to improve the therapeutic response of PTT by enhancing thermal damage deposition and heating selectivity of this strategy while keeping the surrounding normal tissue within the tolerable temperature range. Although, this magnetic targeting approach has shown great success in a small animal model, but further works need to be done to test the reliability of this method on larger animals to prepare it for future clinical applications.

Funding This study was funded by Zahedan University of Medical Sciences (grant number 7970).

Compliance with ethical standards

Conflict of interest The authors declare that they have no conflict of interest.

Ethical approval All applicable international, national, and/or institutional guidelines for the careand use of animals were followed.

References

Abadeer NS, Murphy CJ (2016) Recent progress in cancer thermal therapy using gold nanoparticles. J Phys Chem C 120:4691–4716

Bagher Z, Kamrava SK, Alizadeh R, Farhadi M, Absalan M, Falah M, Faghihi F, Zare-Sadegh A, Komeili A (2018) Differentiation of neural crest stem cells from nasal mucosa into motor neuron-like cells. J Chem Neuroanat 92:35–40

Beik J, Abed Z, Shakeri-Zadeh A, Nourbakhsh M, Shiran MB (2016) Evaluation of the sonosensitizing properties of nano-graphene oxide in comparison with iron oxide and gold nanoparticles. Physica E 81:308–314

Beik J, Khademi S, Attaran N, Sarkar S, Shakeri-Zadeh A, Ghaznavi H, Ghadiri H (2017) A nanotechnology-based strategy to increase the efficiency of cancer diagnosis and therapy: folate-conjugated gold nanoparticles. Curr Med Chem 24:4399–4416

Beik J, Shiran MB, Abed Z, Shiri I, Ghadimi-Daresajini A, Farkhondeh F, Ghaznavi H, Shakeri-Zadeh A (2018) Gold nanoparticle-induced sonosensitization enhances the antitumor activity of ultrasound in colon tumor-bearing mice. Med Phys 45:4306–4314

Chen J, Glaus C, Laforest R, Zhang Q, Yang M, Gidding M, Welch MJ, Xia Y (2010) Gold nanocages as photothermal transducers for cancer treatment. Small 6:811–817

Eustis S, El-Sayed MA (2006) Why gold nanoparticles are more precious than pretty gold: noble metal surface plasmon resonance and its enhancement of the radiative and nonradiative properties of nanocrystals of different shapes. Chem Soc Rev 35:209–217

Eyvazzadeh N, Shakeri-Zadeh A, Fekrazad R, Amini E, Ghaznavi H, Kamrava SK (2017) Gold-coated magnetic nanoparticle as a nanotheranostic agent for magnetic resonance imaging and photothermal therapy of cancer. Lasers Med Sci 32:1469–1477

Farashahi A, Zare-Sadeghi A, Shakeri-Zadeh A, Kamrava SK, Maleki S, Ghaznavi H, Faeghi F (2019) Real-time mapping of heat generation and distribution in a laser irradiated agar phantom loaded with gold nanoparticles using mr temperature imaging. Photodiagn Photodyn Therapy 25:66–73

Ghaznavi H, Hosseini-Nami S, Kamrava SK, Irajirad R, Maleki S, Shakeri-Zadeh A (2018) Folic acid conjugated PEG coated gold–iron oxide core–shell nanocomplex as a potential agent for targeted photothermal therapy of cancer. Artifi Cells Nanomed Biotechnol 46:1594–1604

Hashemian A, Eshghi H, Mansoori G, Shakeri-Zadeh A, Mehdizadeh A (2009) Folate-conjugated gold nanoparticles (synthesis, characterization and design for cancer cells nanotechnology-based targeting). Int J Nanosci Nanotechnol 5:25–34

Jain RK, Stylianopoulos T (2010) Delivering nanomedicine to solid tumors. Nat Rev Clin Oncol 7:653–664

Maeda H, Wu J, Sawa T, Matsumura Y, Hori K (2000) Tumor vascular permeability and the EPR effect in macromolecular therapeutics: a review. J Control Release 65:271–284

Manuchehrabadi N, Toughiri R, Bieberich C, Cai H, Attaluri A, Edziah R, Lalanne E, Johnson AM, Ma R, Zhu L (2013) Treatment efficacy of laser photothermal therapy using gold nanorods. Int J Biomed Eng Technol 12:157–176

Mirrahimi M, Hosseini V, Kamrava SK, Attaran N, Beik J, Kooranifar S, Ghaznavi H, Shakeri-Zadeh A (2018) Selective heat generation in cancer cells using a combination of 808 nm laser irradiation and the folate-conjugated Fe2O3@ Au nanocomplex. Artifi Cells Nanomed Biotechnol 46:241–253

Mirrahimi M, Abed Z, Beik J, Shiri I, Dezfuli AS, Mahabadi VP, Kamrava SK, Ghaznavi H, Shakeri-Zadeh A (2019) A thermo-responsive alginate nanogel platform co-loaded with gold nanoparticles and cisplatin for combined cancer chemo-photothermal therapy. Pharmacol Res. https://doi.org/10.1016/j.phrs.2019.01.005

Qin Z, Bischof JC (2012) Thermophysical and biological responses of gold nanoparticle laser heating. Chem Soc Rev 41:1191–1217

Shakeri-Zadeh A, Eshghi H, Mansoori G, Hashemian A (2009) Gold nanoparticles conjugated with folic acid using mercaptohexanol as the linker. J Nanotechnol Progress Int 1:13–23

Shakeri-Zadeh A, Kamrava SK, Farhadi M, Hajikarimi Z, Maleki S, Ahmadi A (2014) A scientific paradigm for targeted nanophotothermolysis; the potential for nanosurgery of cancer. Lasers Med Sci 29:847–853

Tong L, Wei Q, Wei A, Cheng JX (2009) Gold nanorods as contrast agents for biological imaging: optical properties, surface conjugation and photothermal effects. Photochem Photobiol 85:21–32

Zhao J, Wallace M, Melancon MP (2014) Cancer theranostics with gold nanoshells. Nanomedicine 9:2041–2057

Publisher's Note Springer Nature remains neutral with regard to jurisdictional claims in published maps and institutional affiliations.